# Inhomogeneous width of oxygen-deficient centers induced by electron irradiation of silica

Michele D'Amico,[1,2,*] Fabrizio Messina,[1] Marco Cannas,[1] Maurizio Leone,[1,2] and Roberto Boscaino[1]
[1]*Dipartimento di Scienze Fisiche ed Astronomiche, Università degli Studi di Palermo, Via Archirafi 36, I-90123 Palermo, Italy*
[2]*Istituto di Biofisica, U.O. di Palermo, Consiglio Nazionale delle Ricerche, Via U. La Malfa 153, I-90146 Palermo, Italy*
(Received 4 November 2008; published 18 February 2009)

We report a study of the luminescence activity of oxygen-deficient centers stabilized in as-grown synthetic silica, as compared with the same defects induced by $\beta$ irradiation at increasing doses, ranging from $1.2 \times 10^3$ to $5 \times 10^6$ kGy. We experimentally observe a progressive broadening of the luminescence band with increasing total electron dose released on samples. By analyzing our data within a theoretical model capable of separating homogeneous and inhomogeneous contribution to the total luminescence linewidth, we observe that the increasing of the width is entirely ascribable to the inhomogeneous component which increases, in the most irradiated sample, of 60% with respect to the value in the as-grown sample. This effect can be due either to the progressive creation of new defects statistically exploring different sites of the matrix, or to a progressive structural transformation of silica host which affects the optical properties of induced point defects.

DOI: 10.1103/PhysRevB.79.064203 PACS number(s): 71.55.Jv, 61.80.Fe, 78.55.Qr, 78.47.Cd

## I. INTRODUCTION

Amorphous silicon dioxide or briefly silica ($SiO_2$) is a widely used base material in many different fields, ranging from optical (optical fibers, lenses, fiber Bragg gratings, filters and so on) to electronic technologies (as insulator in metal oxide semiconductor transistors).[1,2] In all these fields, the exposure to ultraviolet (UV), $\beta$ or $\gamma$ radiation results in the creation of point defects inside the matrix.[3] The presence of these defects can either compromise the desired optical or electric features of $SiO_2$ or, in some cases, it can be exploited to tailor the material for specific purposes. For these reasons the study of point defects in irradiated silica is a fundamental technologic issue.[1,2] Moreover, from the general viewpoint of solid-state physics, the comparison between the properties of color centers grown during the production steps, and the same kind of defects induced by irradiation process is an issue of considerable interest, still leaving several unanswered questions especially concerning the understanding of generation mechanisms, that is the distinction between generation processes of defects taking place in random positions of the matrix and those occurring preferentially at precursor sites (e.g., strained bonds, presence of near impurities).[3]

The optical activity of an ensemble of identical defects in a crystalline matrix is representative of the optical fingerprint of the single defect: indeed all defects experience the same local environment due to the virtually perfect translation symmetry of the host. Thus the term *homogeneous* is generally used to refer to the features of a given kind of color center in a crystal. In contrast, in a vitreous system, where many different sites are available for the creation of point defects, those properties related to the whole ensemble of defects are described by the adjective *inhomogeneous*. Hence, in a glass, the overall optical features of an ensemble of point defects belonging to the same "species," such as the line shape of the related absorption or photoluminescence (PL) bands, can be described as a combination of homogeneous properties (controlled by the coupling between electronic transition and phonon modes) and inhomogeneous broadening.[1,2,4] The latter can be regarded as a fingerprint of the underlying amorphous structure hosting the defects. Several experimental evidence has suggested that heavy irradiation can affect the structural properties of silica (e.g., increasing of density, variation of Raman spectra), maybe influencing the inhomogeneous features of the solid as well.[3]

In this paper we study silicon oxygen deficient centers of the second type [Si-ODC(II)] in $SiO_2$, whose structural model was highly debated in the past. The most accepted model is a silicon atom twofold coordinated with two oxygen atoms of the matrix ($=Si^{\bullet\bullet}$).[5–7] The Si-ODC(II) is related to an oxygen deficiency of the material as a consequence of different external perturbations. One of them is the use of an oxygen-poor atmosphere during the synthesis process of the specimen; it is also possible to create ODCs by direct breaking of Si-O linkages or direct knock on of oxygen atoms by high-energy ion implantation,[8–10] or by irradiation with ionizing radiation, such as $\gamma$ rays,[11,12] or heavier $\beta$ rays[12] and neutrons.[13,14] The optical activity of all these Si-ODCs(II) (as-grown defects or induced ones) mainly consists in a broad nearly Gaussian optical-absorption (OA) band centered at $\sim$5.0 eV due to the electronic transition between the ground singlet ($S_0$) and the first-excited singlet ($S_1$) state. The so acquired energy excites a fast (lifetime of $\sim$4 ns) emission band centered at $\sim$4.4 eV, due to the inverse $S_1 \rightarrow S_0$ transition.[7,15] The energy in the $S_1$ level can be released also by a nonradiative process named intersystem crossing (ISC) which populates the first-excited triplet level ($T_1$). This phonon-assisted process produces a slow phosphorescence band centered at $\sim$2.7 eV due to the $T_1 \rightarrow S_0$ transition, which is quenched at temperature below 150 K.[15]

We have recently reported experimental data acquired on ODC(II) by time-resolved luminescence with the aim of developing a technique able to estimate separately the homogeneous and inhomogeneous contributions to the optically measured linewidth of defects in glasses. Data were analyzed within a theoretical model which takes into account the statistical dispersion of geometrical configurations in a glass by introducing a Gaussian distribution of a single homogeneous property of the defects.[16] In this way, we were able to demonstrate that ODCs(II) are strongly affected by inhomoge-

 

TABLE I. First and second column: name and corresponding accumulated $\beta$ dose of investigated samples. Third column: peak position of the photoluminescence emission band. Fourth column: decay lifetime measured at the peak emission energy.

| Name | Dose (kGy) | $E_{peak}$ (eV) | $\tau_0$ (ns) |
|---|---|---|---|
| F300 | As-grown | 4.47 | 4.26 |
| EC1 | $1.2\times10^3$ | 4.41 | 4.08 |
| EC2 | $1.2\times10^4$ | 4.40 | 3.79 |
| EC3 | $1.2\times10^5$ | 4.38 | 4.18 |
| EC4 | $1.2\times10^6$ | 4.38 | 4.95 |
| EC5 | $5.0\times10^6$ | 4.37 | 4.35 |

neous effects, consistently with previous experimental evidences.[17–20]

In this paper we use the same experimental and analysis approach of Ref. 16 to study the luminescence activity of as-grown and $\beta$-ray induced Si-ODC(II). Our aim is to find out if and how defects equilibrated in the matrix during the synthesis process differ from irradiation-induced ones as concerns the inhomogeneous properties. Also, we want to use Si-ODC(II) as a probe to explore the influence of progressive high doses of $\beta$ irradiation on the disorder of the embedding silica matrix. To this purpose, we want to provide an estimation of the inhomogeneous width of Si-ODC(II) as a function of electron irradiation dose.

## II. EXPERIMENTAL SECTION

We report measurements performed on dry synthetic silica (commercial name: Suprasil F300, trademark of Heraeus Quartzglas[21] and cylindrically shaped with 5 mm diameter) with a very low typical concentration of metallic impurities (only a few parts per billion in weight) and low OH content (less than 1 ppm in weight). This material was chosen because it presents a low concentration ($5\times10^{14}$ cm$^{-3}$) of Si-ODC(II), detectable by luminescence measurements, already in the as-grown form. To obtain well measurable PL signals we cut from the as-grown material a slab of 2 mm thickness, hereafter named F300. Other thinner (0.2 mm) five pieces of Suprasil F300 were cut and were $\beta$ irradiated in a Van de Graaff accelerator (2.5 MeV electrons energy) with five different doses, ranging from $1.2\times10^3$ to $5\times10^6$ kGy, as indicated in Table I together with the names hereafter used for these samples. These five samples also feature the luminescence activity related to Si-ODC(II), the intensity of which progressively grows with irradiation dose due to the contribution of radiation-induced centers adding to those present already in the as-grown material.

Photoluminescence measurements were done in a standard back-scattering geometry, under excitation by a pulsed laser (Vibrant OPOTEK: pulse width of 5 ns, repetition rate of 10 Hz, energy density per pulse of $0.30\pm0.02$ mJ/cm$^2$) tuned at 248 nm (5.00 eV), corresponding to the $S_0\rightarrow S_1$ absorption peak of Si-ODC(II). The luminescence emitted by the samples was dispersed by a spectrograph (SpectraPro 2300i, PI Acton, 300 mm focal length) equipped with a 300 grooves/mm grating (blaze at 500 nm) with a spectral bandwidth of 3 nm, and detected by an air-cooled intensified charge-coupled device (CCD) (PIMAX, PI Acton).

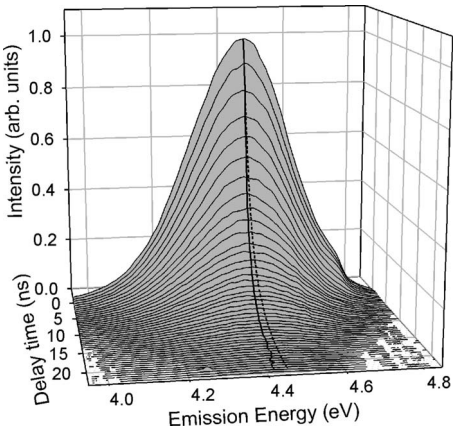


FIG. 1. Time evolution of the line shape of Si-ODC(II) luminescence signals at 25 K excited at ~5 eV in the as-grown F300 sample. The continuous line follows the position of PL peaks whereas the dashed line indicates the peak position of the most intense spectrum at $t=0$ as a guide to the eyes.

The detection system can be electronically gated so as to acquire the emitted signal only in a given temporal window defined by its width ($t_W$) and by its delay $t$ from the laser pulse. The PL decay was followed by performing different acquisitions with the same integration time $t_W=0.5$ ns but at different delays $t$, going from 0 to 30 ns from the laser pulse. All the spectra were corrected for spectrograph dispersion and for instrumental response. All measurements reported here were performed on samples kept at 25 K in high vacuum (~$10^{-6}$ mbar) within a continuous helium flow cryostat (Optistat CF-V, OXFORD Inst.). This temperature was chosen to ensure the absence of nonradiative de-excitation pathways from the excited electronic state, which is to prevent the activation of the ISC process in Si-ODC(II) defects.

## III. RESULTS

We show in Fig. 1 a representative time-resolved measurement of the PL activity of Si-ODC(II) in the F300 as-grown silica sample. The continuous line follows the peak position of the PL band, showing a progressive redshift as a function of delay time from the laser pulse ($t=0$) if compared with the peak position of the first spectrum, reported as well as a reference along all the time scale with a dashed line. Analogous measurements were performed on the EC$n$ series of irradiated samples, where $n$ indicates an integer ranging from 1 to 5 related to the increasing dose of electrons as explained in Table I. In Fig. 2 we report the estimated concentration of Si-ODC(II) defects in all samples. We remark that the main absorption band (centered at ~5 eV) of Si-ODC(II) related to the $S_0\rightarrow S_1$ transition does not undergo remarkable spectroscopic changes because of the irradiation process, but becomes buried by the presence, in this spectral range, of absorption bands related to other

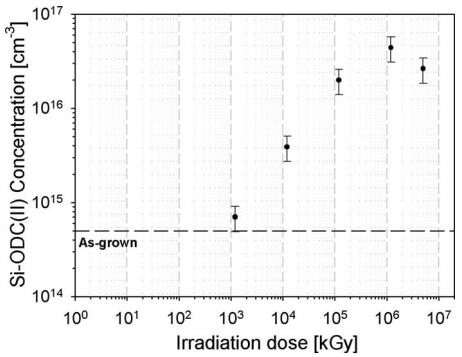


FIG. 2. Concentration of Si-ODC(II) in all investigated samples estimated from luminescence measurements. The dashed line represents the concentration of defects in the as-grown F300 sample.

induced point defects. For this reason, the concentrations of Si-ODC(II) indicated in Fig. 2 have been determined by comparison of the PL intensity of EC*n* samples with the intensity of the luminescence signal in the as-grown F300 sample. Indeed, for this last sample it is possible to obtain the concentration of Si-ODC(II) by the well-known Smakula formula[1] by measuring the absorption coefficient at ~5 eV and using the value $f=0.14$ for the oscillator strength.[22] We observe that the concentration of $\beta$-induced defects in the EC1 sample is comparable to that of as-grown defects in the F300 sample. Thus, to ensure that our considerations about $\beta$-induced defects are not affected by the presence in the irradiated samples of a significant contribution of Si-ODC(II) already present before irradiation, we prefer to neglect this first irradiated sample EC1 and to consider only the rest of samples where the induced Si-ODC(II) concentration is almost one order of magnitude greater than that of as-grown defects. In Fig. 3 panels (a)–(e) we report the PL signal of Si-ODC(II) acquired at $t=0$ in all samples, corresponding to the most intense spectrum reported in Fig. 1 for the F300 sample. In Fig. 3 panels (f)–(j) we report the PL signal of Si-ODC(II) acquired at a delay $t=10$ ns for all samples. The PL band of Si-ODC(II) in the F300 sample, as acquired immediately after the end of the laser pulse, is peaked at $4.45\pm0.02$ eV and features a $0.35\pm0.04$ eV width [full width at half maximum (FWHM)], while the PL bands of irradiated EC*n* samples feature a different peak position (redshifted to $4.35\pm0.02$ eV) and a broader FWHM starting from the EC2 sample ($0.40\pm0.04$ eV) and increasing in the remaining EC3 ($0.41\pm0.04$ eV), EC4, and EC5 samples (both show a $0.44\pm0.04$ eV FWHM). Regarding the spectra acquired after 10 ns from the end of the laser pulse in Fig. 3 panel (f)–(j), they appear redshifted with respect to the corresponding spectra at $t=0$. In particular, the amount of the shift increases along the series of irradiated samples, as can be observed comparing the position of the emission band peaks at $t=10$ ns (vertical solid lines) with that at $t=0$ (vertical dashed lines).

From time-resolved measurements (as that shown in Fig. 1) one can extract the lifetime dispersion curves, namely, the dependence of the decay lifetime $\tau$ from the emission energy. As a representative example we show in Fig. 4 the lifetime dispersion in the EC3 sample.

The lifetimes were obtained by a fitting procedure with a single exponential function of time-resolved PL data at several spectral positions. Hereafter we indicate with the symbol $\tau_0$ the lifetime of each luminescence activity measured at the peak emission energy $E_{peak}$ (as indicated in Fig. 4 for EC3 sample). $E_{peak}$ and $\tau_0$ values estimated for all samples are indicated in Table I.

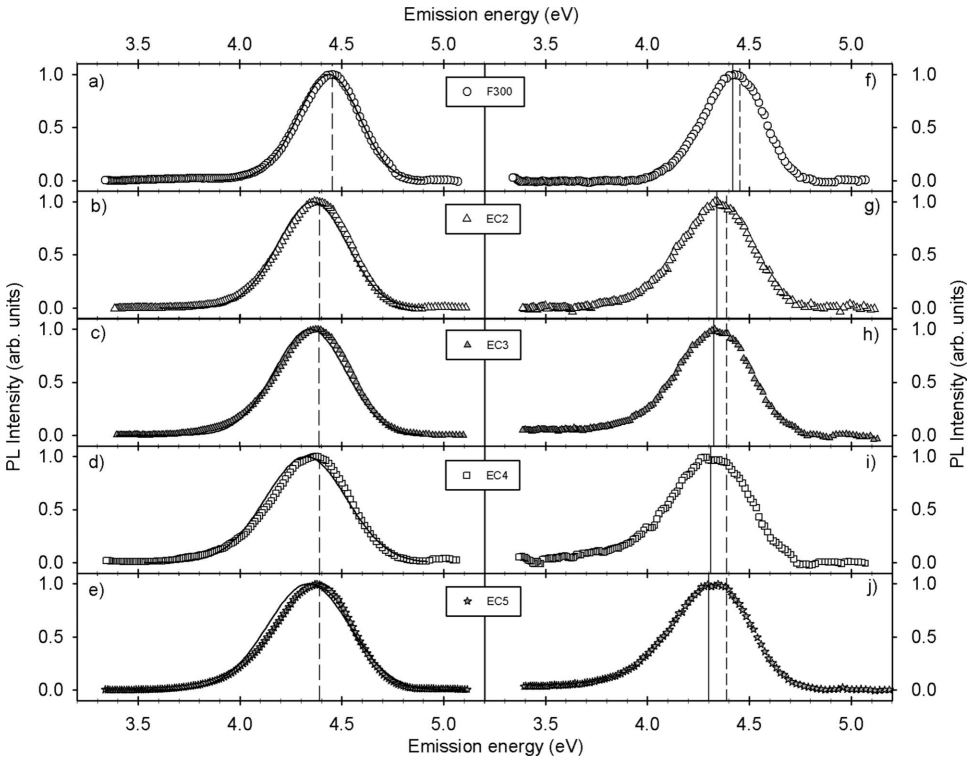


FIG. 3. Luminescence emission line shape of Si-ODC(II) activity as measured at $T=25$ K upon excitation at ~5 eV for all investigated samples. Panel (a)–(e): PL signals acquired immediately after the end of laser pulse ($t=0$). Panels (f)–(j): PL signals acquired at a fixed time delay ($t=10$ ns). The emission-peak positions at $t=0$ (vertical dashed lines) and after a delay of 10 ns (vertical solid lines) are shown. The continuous curves represent the results of the fitting procedure by our theoretical model (see discussion).

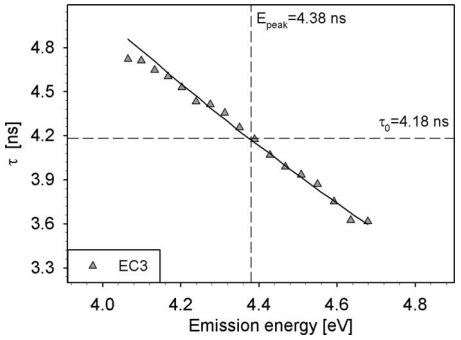


FIG. 4. PL lifetime of Si-ODC(II) in the EC3 sample as a function of the emission energy inside the PL band. The value of the lifetime $\tau_0$ measured at the peak energy of the band $E_{\text{peak}}$ is indicated. The continuous line represents the results of the fitting procedure by our theoretical model (see discussion).

The lifetime of the Si-ODC(II) luminescence in EC3 sample varies from about 4.7 to 3.6 ns for emission energies increasing from about 4.0 to 4.7 eV. This lifetime dispersion is found for all PL activities in all samples, independently from the fact that the defects are already present in the as-grown material (F300 sample) or induced by $\beta$ rays (EC2–EC5). For a better comparison between as-grown and induced defects we show only the results obtained from the decay analysis of F300 and EC5 samples: in Fig. 5 we report the values of the lifetimes $\tau$ in units of $\tau_0$, as a function of the quantity $E$-$E_{\text{peak}}$, i.e., the shift from the peak emission position. In this way the different experimental data are superimposed in the central point with $\tau/\tau_0=1$ and $E$-$E_{\text{peak}}=0$. From Fig. 5 it is clear that induced defects (EC5) feature a greater lifetime dispersion than as-grown ones (F300) evidenced by a greater slope.

The observed energy dependence of the luminescence lifetimes (Figs. 4 and 5) is expected to cause a progressive shift of the first moment[23] $M_1(t)$ of the PL band, due to different temporal evolutions of different parts of the band. From measured spectra we have thus calculated the time dependence of the first moment of the PL band for all samples. For three representative samples (F300, EC3, and EC5) we report in Fig. 6 the values of the decrease (redshift) in the

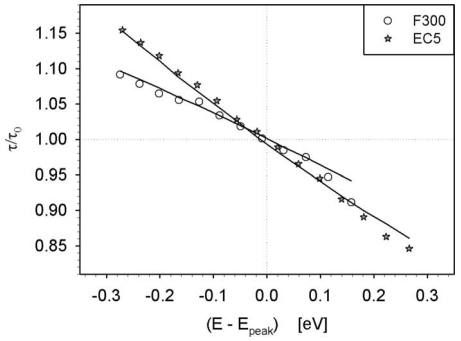


FIG. 5. Lifetime in units of $\tau_0$ as a function of emission energy shifted by $E_{\text{peak}}$ for the luminescence activity of Si-ODC(II) in F300 (as-grown defects) and EC5 samples (induced defects). The continuous lines represent the results of the fitting procedure by our theoretical model (see discussion).

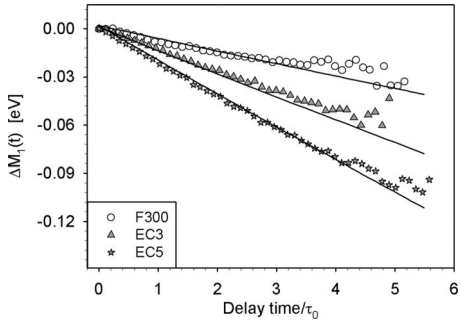


FIG. 6. Difference between first moment at a time delay $t$ and initial first moment at $t=0$ as a function of the time delay in units of $\tau_0$. The continuous lines represent the results of the fitting procedure by our theoretical model (see discussion).

first moment [i.e., $\Delta M_1(t)=M_1(t)-M_1(0)$], as a function of the time delay $t$ in units of $\tau_0$. We observe that all PL activities, both associated to as-grown defects (F300 sample) and to induced defects (EC3 and EC5 samples), feature an approximately linear redshift of the first moment of the band as a function of time. We also note that the slope of this curve, that is the "speed" at which the band shift occurs, is greater in absolute value for induced defects than for as-grown ones. Also, Fig. 6 shows that the curve slope grows as a function of irradiation dose, this being confirmed along all the EC2-EC5 series.[24]

## IV. DISCUSSION

The results found here, which is the distribution of lifetimes measured for different emission energies, and the corresponding redshift of the first moment of the bands as a function of delay time, are in good agreement with analogous results found for similar defects in a previous paper in Ref. 16. In this work we have demonstrated that all these experimental findings are peculiar features of defects embedded in amorphous solid as opposed to defects in crystals, where such effects are not observed. This characteristic behavior of "amorphous defects" can be conveniently referred to as *luminescence dispersion*. These results can be now discussed based on the theoretical model developed in a previous paper.[16] The model is based on the standard background for the description of point defects' optical activities in a solid matrix,[1,25] adding the hypothesis of Gaussian distribution (center $\widehat{E_0}$ and half-width $\sigma_{\text{in}}$) of the zero-phonon energy (ZPE) $E_0$ that is the energy difference between ground- and first-excited electronic states both in the ground vibrational sublevel. This hypothesis models the effect of different environments which can accommodate different members of an ensemble of point defects in an amorphous matrix, and allows to estimate the inhomogeneous and homogeneous half-width, $\sigma_{\text{in}}$ and $\sigma_{\text{ho}}$ respectively, and other homogeneous parameters ($E_0$ and the oscillator strength $f$) by a best fitting procedure. For further details we refer to Appendix.

The behavior shown in Figs. 5 and 6 for both as-grown and radiation-induced Si-ODC(II) PL activities can be examined in the frame of our model. To this aim, for each of the

TABLE II. Upper section: best fitting parameters obtained by our theoretical model for all investigated samples. Lower section: values of λ, $\sigma_{tot}$, $\hbar\omega_p$, and $H$, as calculated from best fitting parameters.

| | $\widehat{E_0}$ (eV) | $\sigma_{in}$ (meV) | $\sigma_{ho}$ (meV) | $f$ |
|---|---|---|---|---|
| F300 | $4.69 \pm 0.05$ | $110 \pm 7$ | $100 \pm 12$ | $0.14 \pm 0.02$ |
| EC2 | $4.64 \pm 0.05$ | $139 \pm 8$ | $94 \pm 11$ | $0.16 \pm 0.02$ |
| EC3 | $4.63 \pm 0.05$ | $141 \pm 8$ | $95 \pm 11$ | $0.15 \pm 0.02$ |
| EC4 | $4.60 \pm 0.05$ | $175 \pm 10$ | $93 \pm 11$ | $0.12 \pm 0.02$ |
| EC5 | $4.61 \pm 0.05$ | $180 \pm 11$ | $90 \pm 11$ | $0.14 \pm 0.02$ |

| | λ(%) | $\sigma_{tot}$ (meV) | $\hbar\omega_p$ (meV) | $H$ |
|---|---|---|---|---|
| F300 | $55 \pm 4$ | $148 \pm 9$ | $37 \pm 7$ | $7 \pm 2$ |
| EC2 | $68 \pm 4$ | $168 \pm 9$ | $29 \pm 6$ | $11 \pm 3$ |
| EC3 | $70 \pm 4$ | $170 \pm 10$ | $29 \pm 6$ | $11 \pm 3$ |
| EC4 | $78 \pm 5$ | $198 \pm 10$ | $28 \pm 6$ | $11 \pm 3$ |
| EC5 | $80 \pm 5$ | $201 \pm 10$ | $26 \pm 5$ | $12 \pm 3$ |

samples listed in Table I (excluding the EC1 sample) we have performed numerical integration varying the above mentioned parameters to obtain a set of three theoretical curves which simultaneously fit the shape of PL bands, the dependence of the decay lifetime vs emission energy and the kinetics of the first moment. The continuous lines in Figs. 3–6 represent the results of our fitting procedure. We obtained a good fit for almost all experimental data especially considering the contemporaneous adaptation of theoretical curves to both temporal and spectral dependences. The slight disagreement between the theoretical curves and experimental data observed in fitting the PL line shape at $t=0$ of the two most irradiated samples (EC4 and EC5), as apparent from Fig. 3, is likely due to the presence of spurious signals at lower energies or to bad approximations in our model (i.e., linear phonon coupling, single mode approximation). However, we observe that also in these two cases the estimation of the parameters $\sigma_{in}$ and $\sigma_{ho}$, which are mainly determined by fitting the lifetime dispersion curve (Fig. 5), and the kinetics of first moment (Fig. 6) are not expected to be affected by the lower quality of the fits of the line shapes. In this work, indeed, our principal aim is to estimate these important parameters ($\sigma_{in}, \sigma_{ho}$) and to find out how and if they depend from the irradiation process.

The upper part of Table II resumes the best parameters obtained by our fitting procedure for all the investigated samples. The values of the oscillator strength found here are in agreement with 0.15 value reported in a review paper about oxygen-deficient centers in silica for the singlet band of Si-ODC(II).[15] From data in the upper part of Table II we can also calculate the Huang-Rhys factor $H=S^2/\sigma_{ho}^2$, the vibrational frequency $\hbar\omega_p=\sigma_{ho}^2/S$ of the effective phonon bath and the total width (from $\sigma_{tot}^2=\sigma_{in}^2+\sigma_{ho}^2$) where $S$ is the half Stokes shift (see Appendix).[16] All these quantities are summarized in the lower part of Table II together with

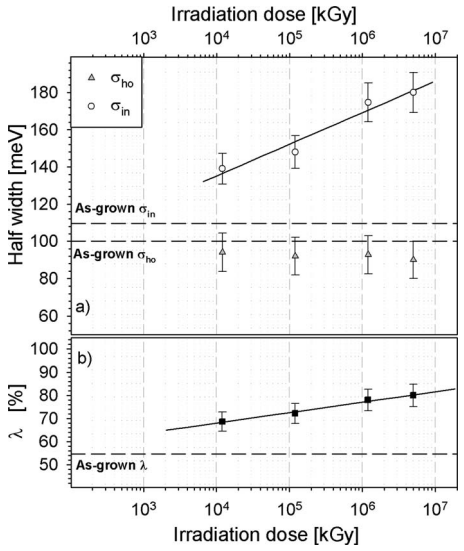


FIG. 7. Homogeneous half-width (gray triangles) and inhomogeneous one (white circles) in panel (a) and parameter λ in panel (b), as a function of $\beta$-irradiation dose in EC$n$ samples. The corresponding values for the as-grown F300 sample are indicated with dashed lines. Continuous lines are a guide to the eyes.

the parameter $\lambda=\sigma_{in}^2/\sigma_{tot}^2$ which estimates the degree of inhomogeneity found in each sample. In Fig. 7 we report the values obtained for the parameters $\sigma_{in}$ and $\sigma_{ho}$ [panel (a)] and for parameter λ [panel (b)], as a function of the $\beta$-irradiation dose for EC$n$ samples, in comparison with the values estimated for the as-grown defects in F300 sample (indicated with dashed lines). We see that the overall degree of inhomogeneity of the ensemble of point defects monotonically increases with irradiation dose, as shown by the behavior of $\sigma_{in}$ and λ parameters. On the other hand, the homogeneous parameter $\sigma_{ho}$ remains almost constant at ~95 meV for induced defects, independently from dose, while being slightly different from the value of ~100 meV characteristic of as-grown defects. A similar behavior is found for the other homogeneous parameters ($\hbar\omega_p, H$) as well as for $\widehat{E_0}$.

All these results can be qualitatively understood as follows: in the as-grown F300 sample, Si-ODC(II) are created in low concentration during the synthesis process and feature well defined homogeneous properties ($\widehat{E_0}=4.69 \pm 0.05$ eV, $\sigma_{ho}=100 \pm 12$ meV, $f=0.14 \pm 0.02$). Such defects are formed in the high-temperature melt state of the silica matrix during the first stage of synthesis, and thus they are stabilized in a configuration which is subsequently frozen when going down to room temperature. Hence, the homogeneous parameters found for the as-grown defects are characteristic of a structural configuration of the center (and of its environment) which is stable at the synthesis temperature. Also, the fact that the degree of inhomogeneity observed in the F300 sample is the lowest in Table II suggests that at high temperatures the defects prefer to form and stabilize in specific precursor sites, likely selected by thermodynamic equilibrium conditions. In this sense, it would be interesting to study how the results on as-grown defects depend on the preparation history of the specimen.

When the $\beta$-irradiation starts, new Si-ODC(II) are created out from the unperturbed silica matrix, so that the concentra-

tion of defects in the EC*n* samples increases as shown in Fig. 2. These centers arise from a totally different mechanism of creation. With so high irradiation doses, we expect Si-ODC(II) to be prevalently created by knock-on events removing oxygen atoms from a normal Si-O-Si bond, followed by a structural rearrangement that accommodates the so-generated local oxygen deficiency in the form of a twofold coordinated silicon atom. In contrast with the as-grown material, in this case the stabilization of the defect and of its environment occurs at room temperature. This allows to understand the spectroscopic differences, apparent from Table II, between the homogeneous parameters of these centers and those of the "high-temperature" ones observed in the as-grown material. In particular, the decrease in the mean vibrational energy for as-grown sample and irradiated ones is in agreement with a previous result on the same defects.[26] Moreover, the spectroscopic distinction between Si-ODC(II) in as-grown silica and Si-ODC(II) created by $\beta$ irradiation had been already put forward in previous works.[11] Based on previous works,[27,28] we argue that these homogeneous differences can be associated to different mean O-Si-O angles between as-grown and induced Si-ODCs(II).

We discuss now the increase in the degree of the inhomogeneity with dose. This finding can be explained by the following simple model. Every site of the matrix can potentially be a precursor for $\beta$-induced generation of Si-ODC(II) activated by knock-on events. However, due to the disorder of the $SiO_2$ matrix, one can expect some Si-O-Si bonds to be "weaker" than others, and to be efficiently activated starting from the lowest irradiation doses. In contrast, other sites where the bond is stronger should be activated only at higher irradiation doses. As a consequence, the inhomogeneous features $(\sigma_{in}, \lambda)$ of the ensemble of $\beta$-induced Si- ODC(II) are not constant with dose: increasing dose allows the growing ensemble of Si-ODC(II) to explore a broader variety of matrix sites, leading to a higher degree of heterogeneity of the environments experienced by the defects, and thus to an increase in $\sigma_{in}$, provided that there is a statistical correlation between the ZPE position and the degree of "toughness" of the precursor sites. This can explain the increase in the inhomogeneity parameter $\lambda$ with dose.

While the above model relies on the assumption of newly formed defects exploring nonequivalent sites within an unperturbed matrix, one has to take into account the possible occurrence of structural transformations of the silica host, progressively involving the volume around the already formed defects as the dose increases. Indeed, it is known that so high irradiation doses induce a measurable densification of the matrix, and the defects have been proposed to play a crucial role in driving this process.[3] The shape of the distribution of the ZPE energy $E_0$ is determined in principle by the detailed dependence of $E_0$ (mapping) from the microscopical structural parameters, which can be elucidated only via suitable quantum-mechanical calculations. Then, we can argue that a progressive distortion of the volume surrounding the defects corresponds to a modification of the statistical distribution of local structural parameters, such as the Si-O-Si angle and the Si-O distances, which may alter in turn the width of the inhomogeneous distribution of the ZPE energy. Such a mechanism could contribute to the observed increase in the $\sigma_{in}$.

Previous experimental evidence has demonstrated the occurrence of significant structural transformations of the silica matrix at very high doses of beta irradiation. For example, in Ref. 29, infrared measurements on heavily irradiated synthetic silica samples revealed variations in the peak position of the intrinsic 2260 $cm^{-1}$ vibration (overtone of a Si-O-Si vibration), which indicated a decrease in the mean Si-O-Si angle taking place upon irradiation. Also, in Ref. 30, Raman measurements allowed to evidence a decrease in the Si-O-Si angular dispersion as well as of the mean Si-O-Si angle, and an increase in the number of three-membered rings, as a consequence of heavy beta irradiation in a variety of silica materials. Hence, the progressive distortion of the silica matrix, clearly proved by such and other papers, surely has to be considered as a mechanism possibly contributing to the observed increase in the inhomogeneous width of the ODC(II) luminescence band. On the other hand, it is worth noting that (see Table II) the homogeneous features of the induced defects do not seem to vary significantly with irradiation dose, as one should expect if the distortion of the embedding matrix strongly affected the defects. Furthermore, data reported in the above papers suggest these distortion effects to be important only for irradiation doses $>10^6$ kGy (corresponding to the two most irradiated samples EC4 and EC5); in contrast, the inhomogeneous width of ODC(II) (see Fig. 7) follows a regular behavior starting from the lowest investigated dose. For these reasons, we feel that both effects (creation of defects in nonequivalent sites and matrix distortion) contribute to the observed increase in the inhomogeneous width, matrix distortion probably being important only at the two highest irradiation doses.

## V. CONCLUSIONS

We studied by time-resolved luminescence the intrinsic oxygen-deficient centers Si-ODC(II) observed in as-grown synthetic amorphous silicon dioxide, and the same defects induced in the same material by $\beta$ irradiation at different doses. The singlet PL of all these defects features a dispersion of decay lifetimes within the emission band and a temporal redshift of the first moment of the band. These experimental findings can be analyzed within a theoretical frame which models the effects induced by disorder in silica. We observe clear differences between the spectroscopic features of the two types of Si-ODC(II). Also, we demonstrate that the degree of inhomogeneity experienced by the induced defects increases with growing irradiation dose and is greater than that experienced by the as-grown centers. These results point to a frame where $\beta$ induced ODC(II) are slightly different from the as-grown ones, likely due to their different formation and stabilization mechanisms. As the irradiation dose increases, the inhomogeneous broadening of the PL band can be due either to the generated defects being able to explore a broader set of geometrical configurations within the silica matrix, or to a global transformation of the host which reflects in a change in the distribution of geometrical parameters and, in turn, to a different distribution of zero-phonon energy.

## ACKNOWLEDGMENTS

We acknowledge financial support received from project "P.O.R. Regione Sicilia - Misura 3.15–Sottoazione C." We are grateful to LAMP research group (http://www.fisica.unipa.it/amorphous/) for support and enlightening discussions. We thank B. Boizot, S. Guillos, and V. Metayer for taking care of the $\beta$ ray irradiation at the Ecole Polytechnique of Palaiseau. The authors would like to thank G. Lapis and G. Napoli for assistance in cryogenic sessions.


## APPENDIX

The homogeneous parameters considered to be undistributed are the half Stokes shift $S$, the homogeneous half-width $\sigma_{ho}$, and the oscillator strength $f$. The parameter $S$, namely, the half-difference between the peak of absorption and luminescence bands, was estimated experimentally by measuring the half-difference between the spectral positions of the excitation energies and emission peaks and thus in following discussion it will be fixed to values $S=0.27$ and 0.31 eV for F300 sample and EC$n$ ones, respectively.

On this basis, one can write a quantitative expression of the PL emitted by the ensemble of color centers in the amorphous solid,[16]

$$L_s(E,t|\widehat{E_0},\sigma_{in},\sigma_{ho},f) \propto \int [E^3 P(E|E_0,\sigma_{ho}) \cdot e^{-t/\tau(E_0,\sigma_{ho},f)}] \cdot e^{-(E_0-\widehat{E_0})^2/2\sigma_{in}^2} dE_0. \quad \text{(A1)}$$

Equation (A1) gives the emission signal $L_s(E,t)$ measured at time $t$ at the spectral position $E$, as obtained by convolution of a Gaussian distribution of $E_0$, whose half-width $\sigma_{in}$ represents the inhomogeneous linewidth of the ensemble of defects, with a homogeneous term (within squared parentheses) representing the PL of a defect emitting at a given value of $E_{em}=E_0-S$ and with homogeneous half-width $\sigma_{ho}$: the spectral shape of the homogeneous term is $E^3P(E|E_0,\sigma_{ho})$, where the $P$ function is a Poissonian with first moment $E_{em}$ and second moment $\sigma_{ho}$. Finally, the radiative lifetime $\tau$ is given by the Forster's equation:[31]

$$1/\tau(E_0,\sigma_{ho},f) = \frac{2e^2n^2}{m_e c^3 \hbar^2} f \int P(E|E_0,\sigma_{ho}) E^3 dE, \quad \text{(A2)}$$

where $n$ is the refractive index of silica considered fixed to value 1.46. One can numerically integrate Eq. (A1) in order to simulate the time-resolved PL spectra, $L_s(E,t)$, as a function of the four parameters $\widehat{E_0}$, $\sigma_{in}$, $\sigma_{ho}$ and $f$. From $L_s(E,t)$ the decay lifetime $\tau_s(E)$ in units of the experimental value $\tau_0$ and the kinetics of the values $M_{1s}(t)$-$M_{1s}(0)$ can be easily calculated by using the same procedure applied to the experimental data $L(E,t)$.

Equation (A2) implies that defects with different emission positions $E_{em}$ within the Gaussian distribution should decay with different lifetimes. In this sense, it immediately allows to understand data in Figs. 5 and 6 on a qualitative basis, if we suppose the PL band of ODC(II) as arising from the inhomogeneous overlap of bands peaked at different energies, statistically distributed within the defect population. For further details we refer to original paper.[16]

*damico@fisica.unipa.it


[1] G. Pacchioni, L. Skuja, and D. L. Griscom, *Defects in SiO$_2$ and Related Dielectrics: Science and Technology* (Kluwer Academic, Dordrecht, USA, 2000).

[2] *Silicon-based Materials and Devices*, edited by H. S. Nalwa (Academic, New York, USA, 2001).

[3] R. A. B. Devine, J.-P. Duraud, and E. Dooryhèe, *Structure and Imperfections in Amorphous and Crystalline Silicon Dioxide* (Wiley, Chichester, UK, 2000).

[4] *Persistent Spectral Hole-Burning: Science and Applications*, edited by W. E. Moerner (Springer-Verlag, Berlin, 1988).

[5] L. Skuja, A. N. Streletsky, and A. B. Pakovich, Solid State Commun. **50**, 1069 (1984).

[6] H. Nishikawa, T. Shiroyama, R. Nakamura, Y. Ohki, K. Nagasawa, and Y. Hama, Phys. Rev. B **45**, 586 (1992).

[7] L. Skuja, J. Non-Cryst. Solids **179**, 51 (1994).

[8] Y. Morimoto, R. A. Weeks, A. V. Barnes, N. H. Tolk, and R. A. Zuhr, J. Non-Cryst. Solids **196**, 106 (1996).

[9] R. H. Magruder III, R. A. Weeks, and R. A. Weller, J. Non-Cryst. Solids **322**, 58 (2003).

[10] M. Hattori, Y. Nishihara, Y. Ohki, M. Fujimaki, T. Souno, H. Nishikawa, T. Yamaguchi, E. Watanabe, M. Oikawa, T. Kamiya, and K. Arakawa, Nucl. Instrum. Methods Phys. Res. B **191**, 362 (2002).

[11] R. Boscaino, M. Cannas, F. M. Gelardi, and M. Leone, Phys. Rev. B **54**, 6194 (1996).

[12] L. Nuccio, S. Agnello, R. Boscaino, B. Boizot, and A. Parlato, J. Non-Cryst. Solids **353**, 581 (2007).

[13] C. M. Gee and M. Kastner, Phys. Rev. Lett. **42**, 1765 (1979).

[14] P. Martín, M. León, and A. Ibarra, Phys. Status Solidi C **2**, 624 (2005).

[15] L. Skuja, J. Non-Cryst. Solids **239**, 16 (1998).

[16] M. D'Amico, F. Messina, M. Cannas, M. Leone, and R. Boscaino, Phys. Rev. B **78**, 014203 (2008).

[17] M. Leone, S. Agnello, R. Boscaino, M. Cannas, and F. M. Gelardi, Phys. Rev. B **60**, 11475 (1999).
[18] A. Cannizzo, S. Agnello, R. Boscaino, M. Cannas, F. M. Gelardi, S. Grandi, and M. Leone, J. Phys. Chem. Solids **64**, 2437 (2003).
[19] A. Cannizzo and M. Leone, Philos. Mag. **84**, 1651 (2004).
[20] A. Cannizzo, M. Leone, R. Boscaino, A. Paleari, N. Chiodini, S. Grandi, and P. Mustarelli, J. Non-Cryst. Solids **352**, 2082 (2006).
[21] Heraeus Quartzglas, Hanau, Germany, catalog POL-0/102/E.
[22] The first moment of a PL band L(E) is calculated with the usual expression $M_1(t)=\frac{\int EL(E,t)dE}{\int L(E,t)dE}$.
[23] The data on EC2 and EC4 samples are not shown in Fig. 6 for sake of drawing clarity because they almost superimposed on data of EC3 and EC5 samples, respectively.
[24] In writing Eq. (A2) we have neglected also the "effective-field correction" term, which can be argued to be close to unity in silica within the investigated spectral range.
[25] A. M. Stoneham, *Theory of Defects in Solids* (Clarendon, Oxford, UK, 1975), Vol. 1.
[26] M. Leone, M. Cannas, and F. M. Gelardi, J. Non-Cryst. Solids **232-234**, 514 (1998).
[27] V. A. Radzig, Chem. Phys. Rep. **14**, 1206 (1995).
[28] A. Cannizzo, S. Agnello, S. Grandi, M. Leone, A. Magistris, and V. A. Radzig, J. Non-Cryst. Solids **351**, 1805 (2005).
[29] G. Navarra, R. Boscaino, M. Leone, and B. Boizot, J. Non-Cryst. Solids **353**, 555 (2007).
[30] B. Boizot, S. Agnello, B. Reynard, R. Boscaino, and G. Petite, J. Non-Cryst. Solids **325**, 22 (2003).
[31] Th. Förster, *Fluoreszenz Organischer Verbindungen* (Vandenhoeck und Ruprecht, Göttinen, 1951), p. 158.